

# COUPLED WAVE-OCEAN MODELLING SYSTEM IN THE MEDITERRANEAN SEA

E. Clementi<sup>1</sup>, P. Oddo<sup>1</sup>, G. Korres<sup>2</sup>, M. Drudi<sup>1</sup> and N. Pinardi<sup>3</sup>

<sup>1</sup>National Institute of Geophysics and Volcanology, Bologna, Italy  
email: [emanuela.clementi@bo.ingv.it](mailto:emanuela.clementi@bo.ingv.it)

<sup>2</sup>Hellenic Centre for Marine Research Institute of Oceanography, Anavyssos, Greece

<sup>3</sup>University of Bologna, Italy

## 1. INTRODUCTION

In the last years, a growing interest has been devoted to wind-wave-current model coupling since their interactions control the boundary fluxes, momentum and energy exchange between the atmosphere and the ocean and within the water column. Model coupling can be achieved at different levels of complexity. In this work we concentrate on wave modifications due to (i) surface current interaction and (ii) effective wind speed correction according to a stability parameter (Tolman, 2002), as well as on the oceanographic parameters changes occurring by (iii) considering a drag coefficient as obtained directly from a wave model.

(i) Wind generated waves can be affected considerably when interact with currents since some particular characteristics of the wave signal, such as wavelength, amplitude, frequency, direction, are modified due to the Doppler shift effect arising from the definition of the absolute wave frequency,  $\omega$ :

$$\omega = \sigma + \mathbf{K} \cdot \mathbf{U} \quad (1)$$

where:  $\mathbf{k}$  is the wave number vector,  $\mathbf{U}$  is the surface current velocity vector, and  $\sigma$  is the wave intrinsic frequency related to the wave number,  $k$ , and water depth,  $d$ , by the dispersion relation:

$$\sigma = \sqrt{gk \tanh kd} \quad (2)$$

that reduces to  $\sigma = \sqrt{gk}$  in deep water. A complete review on wave-current interaction can be found in Jonsson (1990).

(ii) Water temperature, especially sea surface temperature (*SST*), is an important factor to be considered in model coupling because it is very sensitive to the dynamic response of air-sea interaction. *SST* can be accounted in the formulation of the stability correction (Tolman, 2002) by replacing the wind speed with an effective wind speed (increased when unstable) so that the

wave growth reproduces Kahma and Calkoen (1992) stable and unstable growth curves.

(iii) Surface momentum flux (wind stress) is a key element in model coupling since atmospheric winds drive oceanic currents. The stress on the water depends on the wind speed and roughness of the water that relies on surface waves. Estimate of surface wind stress,  $\tau$ , is commonly based on the bulk formula:

$$\tau = \rho_a C_D |\mathbf{U}_{10} - \mathbf{U}| (\mathbf{U}_{10} - \mathbf{U}) \quad (3)$$

where:  $\rho_a$  is the air density,  $C_D$  is the drag coefficient,  $\mathbf{U}_{10}$  is the wind speed at 10m. Uncertainties in wind stress calculation can arise from wind data sampling or resolution and from the choice of the drag coefficient that quantifies how much the surface winds are slowed down because of the wave presence. Several authors have proposed different parameterizations for the drag coefficient usually based on local observations, but for a more realistic computation, explicitly considering the sea state (young wind sea, fully developed wind sea, swell), a wave model should supply an estimate of the drag.

The main objective of this work is to present a coupled modelling system composed by the ocean circulation model OPA-NEMO (Madec et al., 1998; Madec, 2008) and the third-generation wave model WaveWatchIII (WW3) described by Tolman (2009) implemented in the Mediterranean Sea with 1/16° horizontal resolution and forced by ECMWF atmospheric fields. The models are two-way coupled by hourly exchanging the following fields: the sea surface currents and temperature are transferred from NEMO model to WW3 model modifying respectively the wave-current interaction and the wind speed stability parameter; while the drag coefficient computed by WW3 model is passed to NEMO that computes the turbulent component. The performance of the wave model is evaluated by comparing numerical results with buoy measurements for the most common wave fields: significant wave height, mean and peak

periods as well as comparing the significant wave height with remote sensing data. Sea surface numerical currents are also compared with buoy observations.

The paper is organized as follows: section 2 presents the modelling system, its set-up and the sets of measurements used to evaluate the model prediction capability; section 3 illustrates the numerical model results and comparison with observations, and in section 4 the conclusions are described.

## 2. METHODS

The modelling system presented in this work is composed by the coupling of a wave and circulation model as described in the following sections.

Two different sources of data (presented in section 2.5) have been used to assess the ability of the coupled modelling system to improve wave and current fields respect to the uncoupled models for the 1-month study period: January 2013.

### 2.1 THE WAVE MODEL

The wave model used for the simulations is the third generation spectral WaveWatchIII, model version 3.14 (Tolman, 2009), hereafter denoted as WW3. The model solves the wave action balance equation written for a cartesian grid as follows:

$$\frac{\partial N}{\partial t} + \nabla_x \cdot \dot{\mathbf{x}}N + \frac{\partial}{\partial k} \dot{k}N + \frac{\partial}{\partial \theta} \dot{\theta}N = \frac{S}{\sigma} \quad (4)$$

where:  $N(k, \theta, \mathbf{x}, t)$  is the wave action density spectrum defined as the variance density spectrum divided by the intrinsic frequency  $\sigma$ ,  $\theta$  is the wave direction,  $\mathbf{x} = (x, y)$  is the coordinate vector,  $t$  is time and  $S$  represents the net effect of source and sink terms.

Eq. 4 describes the evolution, in slowly varying depth domain and currents, of a 2D ocean wave spectrum where individual spectral component satisfies locally the linear wave theory.

In this work waves interact with surface currents derived from a hydrodynamic model, so the propagation velocity in the different phase spaces can be written as follows:

$$\dot{\mathbf{x}} = \mathbf{c}_g + \mathbf{U} \quad (5)$$

$$\dot{k} = -\frac{\partial \sigma}{\partial d} \frac{\partial d}{\partial s} - \mathbf{k} \cdot \frac{\partial \mathbf{U}}{\partial s} \quad (6)$$

$$\dot{\theta} = -\frac{1}{k} \left[ \frac{\partial \sigma}{\partial d} \frac{\partial d}{\partial m} - \mathbf{k} \cdot \frac{\partial \mathbf{U}}{\partial m} \right] \quad (7)$$

where:  $\mathbf{c}_g$  is the wave propagation velocity vector,  $s$  and  $m$  are the directions respectively along and perpendicular to wave direction.

The source function  $S$  in deep water is represented as a superposition of wind input growing actions  $S_{in}$ , whitecapping dissipation  $S_{ds}$  and nonlinear resonant wave-wave interactions  $S_{nl}$ :

$$S = S_{in} + S_{ds} + S_{nl} \quad (8)$$

In the present application WW3 follows WAM cycle4 model physics (Gunther et al. 1993). Wind input and dissipation terms are based on Janssen's quasi-linear theory of wind-wave generation (Janssen, 1989, 1991); the surface waves extract momentum from the air flow and therefore the stress in the surface layer depends both on the wind speed and the wave-induced stress. The dissipation source term is based on Hasselmann (1974) whitecapping theory according to Komen et al. (1984). The non-linear wave-wave interaction has been modelled using the Discrete Interaction Approximation (DIA, Hasselmann et al., 1985).

### 2.2 THE HYDRODYNAMIC MODEL

The oceanic component of NEMO (Nucleus for European Modelling of the Ocean, Madec et al., 2008) model version 3.4 has been used in the present work.

A description of the operational implementation in the Mediterranean Sea can be found in Oddo et al. (2009) in the framework of the Mediterranean Forecasting System (<http://www.gnoo.bo.ingv.it/mfs/myocean>, Pinardi et al., 2003). The only difference with Oddo's implementation is that the wind stress is computed as the difference between wind and current speed.

### 2.3 MODEL COUPLING

The coupling between wave and circulation models is achieved through an hourly exchange of sea surface current and temperature fields from NEMO to WW3, at the same time WW3 passes to NEMO the drag coefficient. Only when the simulation starts, the models exchange information after the first time step (10 min), since the exchange fields are not included in the restart files. A sketch of the coupling mechanism is represented in Fig. 1.

In particular sea surface temperature field is used to evaluate a stability parameter in the formulation of the effective wind speed correction as presented in Tolman (2002):

$$u_e = u \left( \frac{c_0}{1 \pm c_1 \tanh[\pm c_2 (Stab - Stab_0)]} \right)^{1/2} \quad (9)$$

where:  $c_0$ ,  $c_1$ ,  $c_2$  and  $Stab_0$  are set respectively equal to 1.4, 0.1, 150, -0.01 and the sign is the same of  $(Stab - Stab_0)$ . The stability factor  $Stab$  is calculated as in Tolman (2002) and depends on air-sea temperature difference.

Drag coefficient evaluated by WW3 is passed to the circulation model where it is updated with its turbulent part following Large and Yeager (2004) and Large (2006) formulation and the full wind stress  $\tau$  is evaluated as expressed in Eq. 1.

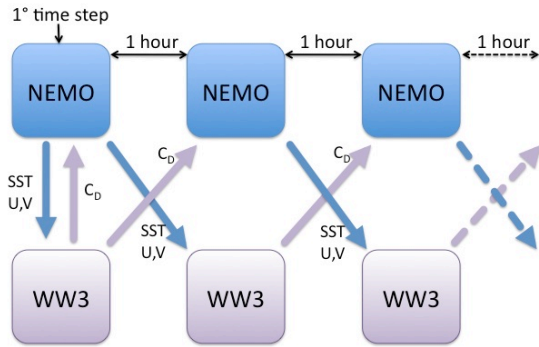


Figure 1. Sketch of the coupling mechanism between WW3 and NEMO. When the simulation starts, models exchange information at the first time step (10 min), while later they communicate every hour. NEMO sends to WW3 sea surface temperature ( $SST$ ) and current fields ( $U, V$ ), while WW3 passes to NEMO the drag coefficient ( $C_D$ ).

## 2.4 EXPERIMENTS SET-UP

Three numerical experiments have been carried out for the period January 2013 by implementing the

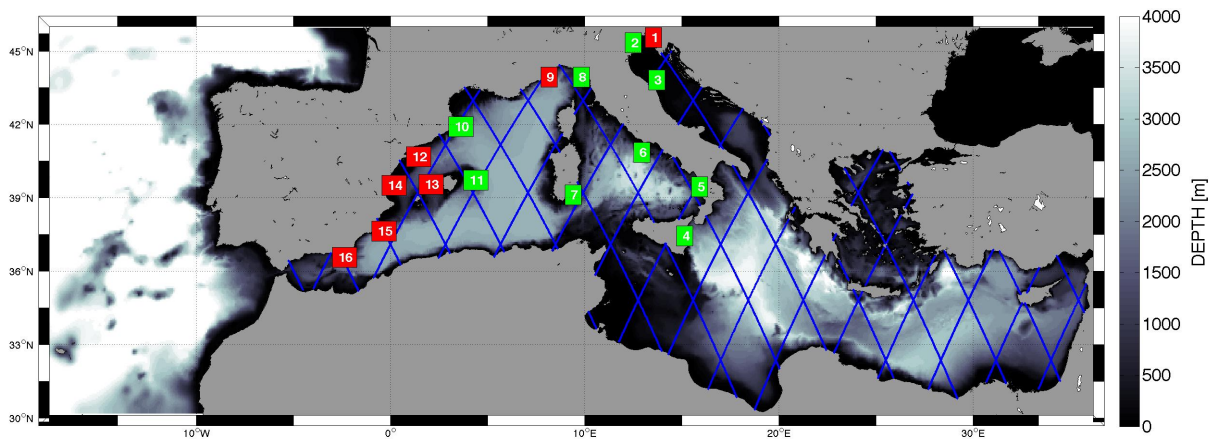


Figure 2. Representation of the model domain and bathymetry: Mediterranean Sea extended to the Atlantic. Red squares represent location of buoys measuring wave and current data, green squares represent position buoys measuring only wave data. Blue lines refer to altimeter Jason-2 tracks for the period January 2013. Buoys notation and corresponding names are listed in Table 1.

NEMO-WW3 numerical modelling system in the Mediterranean Sea domain extended into the Atlantic as represented in Figure 2. Both models are defined on the same grid with  $1/16^\circ$  horizontal resolution, NEMO vertical resolution is defined by 72 unevenly spaced z-levels using partial cells to fit the bottom depth shape while for the wave model the spectral discretization is achieved through 30 frequency bins ranging from 0.05 Hz (corresponding to a period of 20 s) to 0.79 Hz (corresponding to a period of about 1.25 s) and 24 equally distributed directional bins ( $15^\circ$  directional increment).

The models are both forced by the 6h,  $1/2^\circ$  horizontal resolution operational analyses from the European Centre for Medium-Range Weather Forecasts (ECMWF).

The three experiments are set as follows:

- WW3 uncoupled: the wave model standalone not using sea surface currents and temperature derived from the circulation model, meaning no wave-current interaction and wind correction are performed in this experiment;
- NEMO uncoupled: the hydrodynamic model standalone, where the drag coefficient has been calculated in the model using the Hellerman and Rosenstein (1983) formulation depending on the air-sea temperature difference and the wind speed;
- WW3-NEMO coupled: the two models are two-way coupled by hourly exchanging parameters as described in previous section 2.3.

Table 1. Wave and current buoys notation as represented in Figure 1.

n.	Buoy name	n.	Buoy name	n.	Buoy name	n.	Buoy name
1	Vida	5	Cetraro	9	Capo Mele	13	Tarragona
2	Venezia	6	Cagliari	10	Cabo Begur	14	Valencia
3	Ancona	7	Ponza	11	Mahon	15	Cabo de Palos
4	Catania	8	La Spezia	12	Dragonera	16	Cabo de Gata

## 2.5 OBSERVATIONS

Two sets of data have been used to evaluate the accuracy of the model results.

The first source of data consists of daily averages of in-situ observations deriving from the Mediterranean CalVal buoys network (Tonani et al., 2012; <http://gnoo.bo.ingv.it/myocean/calval/>).

The second set of data is composed by satellite altimeter-derived wave heights from OSTM/Jason-2 (CNES–NASA). Jason-2 is a low-orbit satellite, equipped with high-precision ocean altimetry that measures the distance between the satellite and the ocean surface, within a few centimetres. The recommended calibrated significant wave height data (with corrections applied to the altimeter 1Hz estimates values) have been used. The comparison has been evaluated by choosing the closest grid point to the buoy station or the satellite track.

Figure 2 represents satellite tracks and spatial location of buoys, distinguishing between buoys measuring only wave fields (green squares) and the ones measuring also hydrodynamic characteristics (red squares). Buoys notation and corresponding names are listed in Table 1.

## 3. RESULTS AND DISCUSSION

The ability of the models to represent observations is evaluated by means of standard statistics such as: bias ( $B$ ), root mean square error ( $RMS$ ), normalized standard deviation ( $STN$ ), and correlation coefficient ( $R$ ):

$$B = \frac{1}{N} \sum_{i=1}^N (M_i - O_i) \quad (10)$$

$$RMS = \sqrt{\frac{1}{N} \sum_{i=1}^N (M_i - O_i)^2} \quad (11)$$

$$STDN = \frac{\sigma_M}{\sigma_O} = \frac{\sqrt{\sum_{i=1}^N (M_i - \bar{M})^2}}{\sqrt{\sum_{i=1}^N (O_i - \bar{O})^2}} \quad (12)$$

$$R = \frac{\sum_{i=1}^N (M_i - \bar{M})(O_i - \bar{O})}{\sqrt{\frac{1}{N} \sum_{i=1}^N (M_i - \bar{M})^2 (O_i - \bar{O})^2}} \quad (13)$$

where:  $M$  represents the model results and  $O$  the observations,  $N$  is the number of data and the overbar characterizes the mean value.

This section is organized in two parts: the first describes the wave model results comparison with buoy and altimeter data, and the second shows the circulation model results comparison with buoys in terms of sea surface currents.

### 3.1 WW3 MODEL RESULTS

Results of WW3 uncoupled and coupled experiments have been first compared to buoy measurements by means of daily averages. Table 2 summarizes the main statistics (bias, root mean square error, normalized standard deviation and correlation coefficient) of significant wave height (WH), mean period (TM) and peak period (TP) model results. In almost all cases (except for the mean period bias), WW3-NEMO coupled model better reproduces buoy measurements if compared to the WW3 uncoupled model results. It is evident that numerical significant wave height and peak period underestimate observations and are characterized by lower variation, while predicted mean period is in average larger than data and more dispersed. In general wave height is better forecasted by the models respect to the periods, being characterized by a high value of the correlation coefficient.

Table 2. Statistics evaluated from the comparison between buoy measurements and model results in terms of wave height (WH), mean period (TM) and peak period (TP) for uncoupled and coupled wave model.

	WH uncoupled	WH coupled	TM uncoupled	TM coupled	TP uncoupled	TP coupled
<b>Bias</b>	-0.29 m	-0.24 m	0.24 s	0.26 s	-0.56 s	-0.54 s
<b>RMS</b>	0.42 m	0.39 m	0.85 s	0.83 s	1.50 s	1.46 s
<b>STDN</b>	0.82	0.84	1.26	1.25	1.06	1.05
<b>Correlation</b>	0.92	0.92	0.75	0.76	0.72	0.73

Previous observations are then clarified in Figures 3a,b,c showing scatter plots of buoy measurements respect uncoupled (red) and coupled (blue) model results for January 2013. The regression lines of both buoy data versus uncoupled and coupled models are also plotted in order to represent the distance from a best-fit (1:1) line. Comparison of significant wave heights (Figure 3a) confirms that both numerical experiments underestimate buoy data, regression lines are steeper than the best-fit line and have positive intercepts, in particular coupled model suits better in-situ observations if compared to the uncoupled one. Mean period comparison is represented in Figure 3b showing a larger scatter respect to significant wave height data. Coupled model presents only a slightly better fit if compared to the uncoupled one and in both cases regression lines have lower slopes than the best-fit line and positive intercepts. As shown in Figure 3c peak period slightly improves if the wave model is coupled with the circulation model. In particular both model experiments underestimate buoys peak period, have less steep regression line respect to the best-fit line and positive intercept.

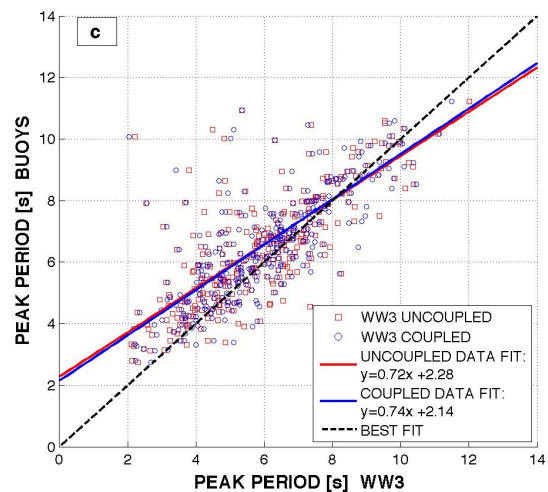
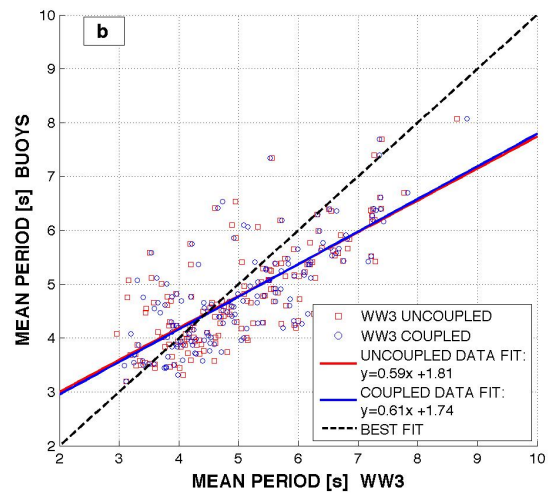
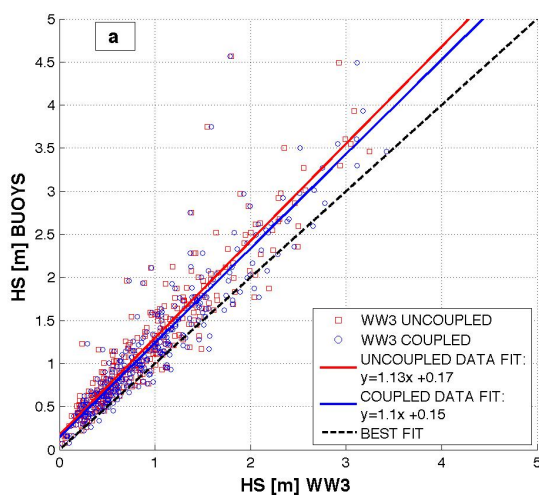


Figure 3: Scatter plot for the study period January 2013 of: a) significant wave height, b) mean period and c) peak period comparison between buoy data and numerical WW3 uncoupled (red) and coupled (blue) model results. Black dashed line represents the the best-fit (1:1) line, red line is the buoy-uncoupled model data fit, while blue line shows the buoy-coupled model data fit.

Daily averaged significant wave height and peak period time series of the Ancona buoy (black line), represented here as a reference station, is plotted in Figure 4 together with uncoupled (red line) and coupled (blue line) model results. As already mentioned, these plots highlight that both experiments underestimate wave height,

particularly higher values, as well as peak period measurements. Main statistics listed in the plots confirm that model predictions are in accordance with observations, and the WW3-NEMO coupled model better reproduces buoy data if compared to the WW3 uncoupled model experiment.

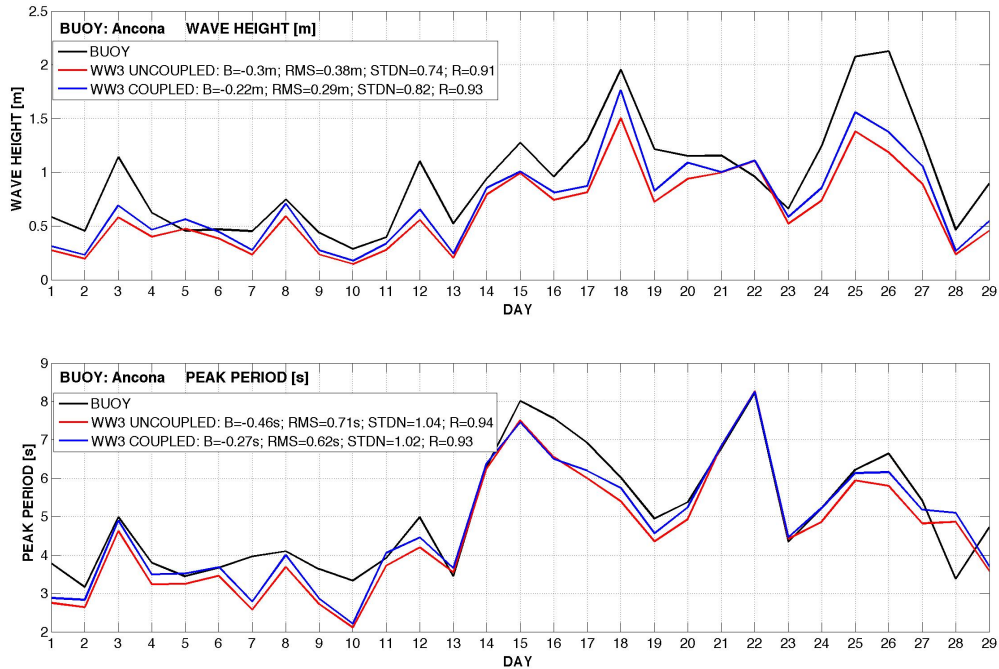


Figure 4: Daily averages of significant wave height (top panel) and peak period (bottom panel) for January 2013 referred to the Ancona buoy. Black line represents buoy data, red line corresponds to WW3 uncoupled model and blue line is referred to WW3-NEMO coupled model. Main statistics are listed in the pictures.

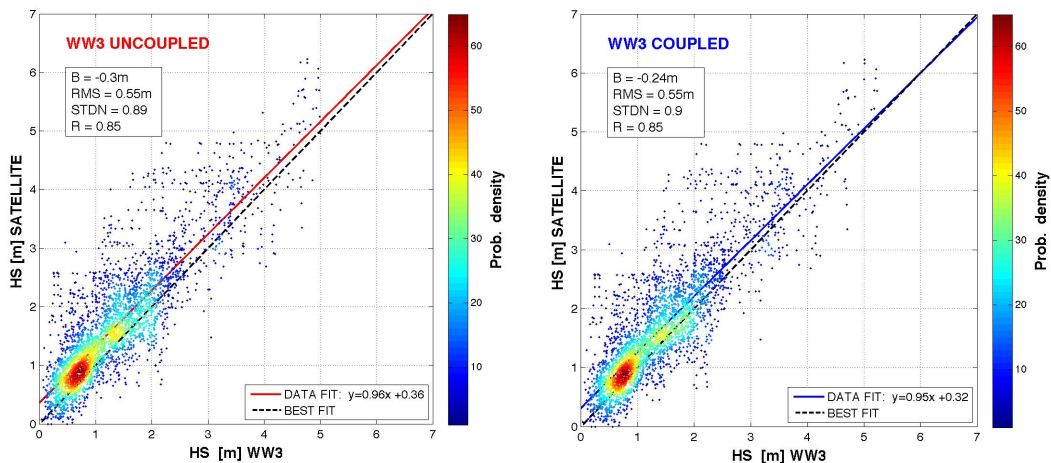


Figure 5: Scatter plot of significant wave height (HS) comparison between Jason2 satellite data and numerical results for January 2013. Left panel represents WW3 uncoupled model results: main statistics between the 2 sets of data are:  $B=-0.30\text{m}$ ,  $\text{RMS}=0.55\text{m}$ ,  $\text{STDN}=0.89$  and  $R=85\%$ . Right panel shows WW3-NEMO coupled model results: main statistics between the 2 set of data are:  $B=-0.24\text{m}$ ,  $\text{RMS}=0.55\text{m}$ ,  $\text{STDN}=0.90$  and  $R=85\%$ . Point colours refer to the data probability density; black dashed line represents the best-fit (1:1) line, solid lines show the satellite-model data fit.

Since the performance of the wave models is different in the open sea and close to the coasts, a second set of measures has been considered: significant wave height as measured by the altimeter Jason-2 data. Similarly to what has been done for buoys, Figure 5 (left: WW3 uncoupled results, right: WW3-NEMO coupled results) shows how the model results fit altimeter data, different colours are used to represent the data density, in particular larger data concentration is found at 1m significant wave height. Main statistics are listed in the figure showing that, also in this case, numerical significant wave height underestimates the ones measured by the altimeter and presents lower standard deviation. The WW3-NEMO coupled system confirms to be closer to the observations if compared to the uncoupled model. Considering root mean square error and correlation coefficient, we can notice that model comparison with satellite data has lower skill respect to buoy comparison.

### 3.2 NEMO MODEL RESULTS

Daily averaged surface currents as calculated by the two sets of experiments, namely NEMO uncoupled and WW3-NEMO coupled model, are compared to buoy measurements in order to assess the skill and the improvement achieved by the coupled system.

Table 3 summarizes main statistics derived from the comparison of model results and buoy data, showing that similar results are achieved by the two experiments: model predictions underestimate measurements, have larger deviation than observations and a low correlation coefficient. In particular they presents the same bias and root mean square error, while the coupled model standard deviation is slightly more comparable to that calculated using observations. Considering the large error and the poor correlation between model results and buoy measurements, the coupling with the wave model doesn't enhance the capability of NEMO model to predict surface currents in proximity of the coasts that still remains poor.

Table 3. Statistics evaluated comparing buoy velocity current measurements and model results from uncoupled and coupled circulation model.

	<b>Current uncoupled</b>	<b>Current coupled</b>
<b>Bias</b>	-0.05 m/s	-0.05 m/s
<b>RMS</b>	0.18 m/s	0.18 m/s
<b>STDN</b>	1.31	1.27
<b>Correlation</b>	0.15	0.16

## 4. CONCLUSIONS

A new coupled wave-current (WW3-NEMO) model system, consisting in a hourly two-way exchange of parameters among the two models, has been implemented in the Mediterranean Sea and presented in this work. In order to evaluate the performance of the coupled model, three sets of experiments have been performed, namely: WW3 uncoupled, NEMO uncoupled and WW3-NEMO coupled, and compared to buoy measurements and satellite altimeter Jason-2 data for the January 2013 period. All the wave experiments proved to have good skill in reproducing both in situ and satellite measured wave parameter, pointing out that the coupled modelling system can improve the already good results achieved by standalone wave model. In particular wave model better predicts wave height in the vicinity of the coasts and measured by buoys respect to the satellite altimeter wave heights covering a wider area of measurement.

A lower improvement has also been reached by comparing coupled and uncoupled circulation model sea surface velocities and buoy observations, but circulation model prediction capability still remains poor.

Further research and analysis of a larger dataset for a longer period should be useful to assess more accurate conclusions. However, this work suggests that a two-way coupled model might be capable of an improved description of wave-current interactions, in particular feedback from the ocean to the waves might assess an improvement on the prediction capability of wave characteristics.

### ACKNOWLEDGEMENTS

This work was supported by the European Commission MyOcean2 Project (SPA.2011.1.5-01; development of upgrade capabilities for existing GMES fast-track services and related operational services; Grant Agreement 283367, FP7-SPACE-2011).

### REFERENCES

- Gunther, H., H. Hasselmann, and P.A.E.M. Janssen, 1993: The WAM model cycle 4, DKRZ report n. 4.
- Hasselmann, K., 1974: On the characterization of ocean waves due to white capping, *Boundary-Layer Meteorology*, **6**, 107-127.
- Hasselmann, S. and K. Hasselmann, 1985: Computations and parameterizations of the nonlinear energy transfer in a gravity wave spectrum. Part I: A new method for efficient computations of the exact

- nonlinear transfer integral, *J. Phys. Ocean.*, **15**, 1369-1377.
- Hasselmann, S., K. Hasselmann, J. H. Allender, and T.P. Barnett, 1985: Computations and parameterizations of the nonlinear energy transfer in a gravity wave spectrum. Part II: Parameterizations of the nonlinear energy transfer for application in wave models, *J. Phys. Ocean.*, **15**, 1378-1391.
- Hellerman, S. and M. Rosenstein, 1983: Normal monthly wind stress over the world ocean with error estimates, *J. Phys. Ocean.*, **13**, 93-104.
- Janssen, P.A.E.M., 1989: Wave induced stress and the drag of air flow over sea wave, *J. Phys. Ocean.*, **19**, 745-754.
- Janssen, P.A.E.M., 1991: Quasi-Linear theory of wind wave generation applied to wave forecasting, *J. Phys. Ocean.*, **21**, 1631-1642.
- Jonsson, I.G., 1990: Wave-current interactions. In B. Le Mehaute and D.M. Hanes (Eds), *The Sea*, *Ocean Engineering Science*, **9**, 65-120, Wiley, New York.
- Kahma, K.K. and C.J. Calkoen, 1992: Reconciling discrepancies in the observed growth of wind-generated waves. *J. Phys. Ocean.*, **22**, 1389-1405.
- Komen, G. J., S. Hasselmann, and K. Hasselmann, 1984: On the existence of a fully developed windsea spectrum, *J. Phys. Ocean.*, **14**, 1271-1285.
- Large, W. and S. Yeager, 2004: Diurnal to decadal global forcing for ocean and sea-ice models: the data sets and flux climatologies. CGD Division of the National Center for Atmospheric Research, NCAR Technical Note: TN-460+STR, NCAR, 111 pp.
- Large, W., 2006: Surface Fluxes for Practitioners of Global Ocean Data Assimilation, in *Ocean Weather and Forecasting*. Ed. E. Chassignet and J. Verron, Springer, 229-270.
- Madec, G., P. Delecluse, M. Imbard, and C. Levy, 1998: OPA version 8.1 ocean general circulation model reference manual, Technical Report, LODYC/IPSL, Note **11**, Paris, France, 91 pp.
- Madec, G., 2008: NEMO ocean engine. Note du Pole de modélisation, Institut Pierre-Simon Laplace (IPSL), France, Note **27** ISSN 1288-1619, 209 pp.
- Oddo, P., M. Adani, N. Pinardi, C. Fratianni, M. Tonani, and D. Pettenuzzo, 2009: A nested Atlantic-Mediterranean Sea general circulation model for operational forecasting, *Ocean Sci.*, **5**, 461-47.
- Pinardi, N., I. Allen, P. De Mey, G. Korres, A. Lascaratos, P.Y. Le Traon, C. Maillard, G. Manzella, and C. Tziavos, 2003: The Mediterranean Ocean Forecasting System: first phase of implementation (1998-2001). *Ann. Geophys.*, **21**, 3-20.
- Tolman, H.L., 2002: Validation of WAVEWATCH III version 1.15 for a global domain. NOAA / NWS / NCEP / OMB Technical Note **213**, 33 pp.
- Tolman, H.L., 2009: User manual and system documentation of WAVEWATCH III™ version 3.14. NOAA/NWS/NCEP/MMAB Tech. Note **276**, 194 pp.
- Tonani M., J.A.U. Nilsson, V. Lyubartsev, A. Grandi, A. Aydogdu, J. Azzopardi, G. Bolzon, A. Bruschi, A. Drago, T. Garau, J. Gatti, I. Gertman, R. Goldman, D. Hayes, G. Korres, P. Lorente, V. Malacic, A. Mantziafou, G. Nardone, A. Olita, E. Ozsoy, I. Pairaud, S. Pensieri, L. Perivoliotis, B. Petelin, M. Ravaioli, L. Renault, S. Sofianos, M.G. Sotillo, A. Teruzzi, and G. Zodiatis, 2012: Operational evaluation of the Mediterranean Monitoring and Forecasting Centre products: implementation and results. Poster at the JCOMM-4 workshop, Yeosu, Korea Rep. 2012.